Scalar and Representative Observables for Polarimetric SAR Data

Thanh-Hai Le, Ian McLoughlin, and Chan-Hua Vun

Abstract—This paper presents several novel scalar statistical models to represent the determinant of both partial and full polarimetric SAR (POLSAR) covariance matrices. Compared to other scalar statistical models for POLSAR, the proposed models are highly representative of the multi-dimensional data and enable useful discrimination measures to be easily determined. The representative power of these models is explained when these multi-dimensional models are collapsed to single dimensional versions, they are shown to exactly match the traditional statistical models for the representative observable of SAR intensity. The paper also validates the theoretical models together with their derived discrimination measures using real world POLSAR data. One major benefit of this paper is that these proposed generic models can facilitate the adaptation of existing SAR techniques to higher-dimensional POLSAR data. To illustrate, an example is given where the determinant-ratio and its additive version, contrast, are applied in the evaluation of POLSAR speckle filters.

Index Terms—Polarimetric Synthetic Aperture Radar, Electromagnetic Modeling, Multidimensional Signal Processing

I. Introduction

During the past decades, exponential growth in computing power has allowed once computationally-demanding Synthetic Aperture Radar (SAR) technology to become a feasible and preferred technique for earth observation applications. SAR technology has since extended in a few directions, one of which is polarimetric SAR (POLSAR). POLSAR extends SAR by exploiting the natural polarization property of Electro-Magnetic (EM) waves, leading to the availability of multi-channel POLSAR data, compared to traditional one-channel SAR data.

While statistical models are important in understanding the stochastic nature of both SAR and POLSAR, in extending our understanding towards multi-dimensional POLSAR, an important issue needs to be addressed. That is there now exists not one but many observable quantities in multi-channel POLSAR (as opposed to single-channel SAR intensity). The research community has responded largely by developing different statistical models for various POLSAR observables. However for a statistical model to be useful, scalar discrimination measures generally need to be derivable from it. Thus, practical applications for POLSAR data processing require dis-similarity measures that are scalar, consistent and preferably homoskedastic on the one hand. On the other hand,

Thanh-Hai Le and Chan-Hua Vun are with School of Computer Engineering, Nanyang Technological University, Singapore. Ian McLoughlin is with School of Information Science and Technology, University of Science and Technology of China.

the observable quantity being modelled should be naturally representative of the high dimensionality POLSAR data.

This paper presents novel statistical models for multi-channel POLSAR data as generalisations of the commonly used and representative statistical models for the one-channel SAR data. This approach makes feasible the adaptation of many existing SAR processing techniques to be applied to POLSAR data. After section II reviews related work in published literature, statistical models for the heteroskedastic POLSAR determinant and its homoskedastic log-domain equivalent, together with several other discrimination measures are derived in section III. The representative properties of these observables are then demonstrated in section IV where the multi-dimensional POLSAR data is collapsed to a one-dimensional SAR scenario. With this transformation, the determinant of the POLSAR covariance matrix is shown to be equivalent to SAR intensity, and allow many conventional SAR statistical models to stay under the umbrella of these generic POLAR models. The proposed theoretical models are then validated against real life practical data in section V. Section VI briefly describes how evaluation of an existing SAR data processing technique, the speckle filter, can be extended to POLSAR data processing using this approach. This is followed by a conclusion in Section VII.

II. Related Work in Literature

This section outlines related published work. In particular, section II-A reviews various scalar statistical models used for different POLSAR observables. Its purpose is to show that none of those models have led to statistically consistent discrimination measures. Section II-B further strengthens those findings by discussing discrimination measures that have been proposed for POLSAR, and demonstrates that almost all of them are based on the likelihood statistical test for complex Wishart distribution. However, while an exact statistical distribution is needed for the test, only asymptotic distribution is used in the original work [1].

A. Scalar Observables for POLSAR Data and their Statistical Models

Different target decomposition theorems have identified many possible scalar observables for complex POLSAR data. In [2], the performance of different scalar POLSAR observables is evaluated for classification purposes. While many scalar observables for POLSAR were presented, their corresponding statistical models and classifiers were not available. Furthermore, at its conclusion, the paper indicated that it is

impossible to identify a single best representation. Although, to be fair, those observables were identified to describe a decomposed portion of the complex POLSAR data, rather than providing a single unified representation of the POLSAR data.

Given that the joint distribution for POLSAR is known to be the multi-variate complex Wishart distribution, it is possible to derive the scalar statistical models for some univariate POLSAR observables. This becomes an alternative approach used in the study of POLSAR data. However, such derivations are no trivial task, and so far, only a handful of such statistical models have been proposed, including the following:

1) cross-pol ratio $r_{HV/HH} = |S_{HV}|^2/|S_{HH}|^2$ [3],
2) co-pol ratio $r_{VV/HH} = |S_{VV}|^2/|S_{HH}|^2$ [3],
3) co-pol phase difference $\phi_{VV/HH} = arg(S_{VV}S_{HH}^*)$ [3] [4],
4) magnitude $g = |avg(S_{pq}S_{rs}^*)|$ [4],
5) normalized magnitude $\xi = \frac{|avg(S_{pq}S_{rs}^*)|}{\sqrt{avg(|S_{pq}|^2)avg(|S_{rs}|^2)}}$ [4],
6) intensity ratio $w = avg(|S_{pq}|^2)/avg(|S_{rs}|^2)$ [4],
7) and the Stokes parameters $S_i, 0 \le i \le 3$ [5].

More recently, statistical models for each element of the POLSAR covariance matrix $S_{pq}S_{rs}^*$ [6] as well as for the largest eigen-value of the covariance matrix λ_1 [7] have been proposed. While these models undoubtedly help in understanding POLSAR data, none of these observables have been shown to meet the dual criteria of 1) resulting in statistically consistent discrimination measures and 2) being representative of the complex POLSAR data.

B. POLSAR Discrimination Measures

The commonly used measure of distance for matrices are either the Euclidean or Manhattan distances, defined as:

$$d(C_x, C_y) = \sum_{i,j} |\mathbb{R}(C_x - C_y)_{i,j}| + \sum_{i,j} |\mathbb{I}(C_x - C_y)_{i,j}| \quad (1)$$

$$d(C_x, C_y) = \sqrt{\sum_{i,j} |C_x - C_y|_{i,j}^2} \quad (2)$$

where $C_{i,j}$ denotes the (i,j) elements of the POLSAR covariance matrix C, $||$ denotes absolute values and $\mathbb{R}, \mathbb{I}$ denote the real and imaginary parts respectively. However, in the context of POLSAR, these dis-similarity measures are not widely used mainly due to the multiplicative nature of the noisy data.

In the field of POLSAR, the Wishart distance is probably the most widely used, as part of the well-known Wishart classifier [8]. It is defined [9] as:

$$d(C_x, C_y) = \ln |C_y| + tr(C_x C_y^{-1}) \quad (3)$$

, where $tr(C)$ denotes the trace of the matrix C. As a measure of distance, its main disadvantage is that $d(C_y, C_y) = \ln |C_y| \neq 0$.

Recent works have suggested alternative dissimilarity measures including the symmetric and asymmetric refined Wishart distance [10],

$$d(C_x, C_y) = \frac{1}{2}tr(C_x^{-1}C_y + C_y^{-1}C_x) - d \quad (4)$$

$$d(C_x, C_y) = \ln |C_x| - \ln |C_y| + tr(C_x C_y^{-1}) - d \quad (5)$$

the Bartlett distance [11],

$$d(C_x, C_y) = 2\ln |C_{x+y}| - \ln |C_x| - \ln |C_y| - 2d\ln 2 \quad (6)$$

the Bhattacharyya distance [12],

$$r(C_x, C_y) = \frac{|C_x|^{1/2}|C_y|^{1/2}}{|(C_x + C_y)/2|} \quad (7)$$

and the Wishart Statistical test distance [13]

$$d(C_x, C_y) = (L_x + L_y)\ln |C| - L_x \ln |C_x| - L_y \ln |C_y| \quad (8)$$

.

Closer investigation of these dis-similarity measures reveals that most are related in some ways. The Bhattacharyya distance is easily shown to be related to the Barlett distance. At the same time the Barlett distance can be considered a special case of the Wishart Statistical Test distance, when the two data sets have the same number of looks, i.e. $L_x = L_y$. The close relation among the measures is further supported by the fact that all of their proposing papers refered the same statistical model developed in [1] as a foundation. In [1], to determine if the two scaled multi-look POLSAR covariance matrix Z_x and Z_y, which have L_x and L_y as the corresponding number of looks, come from the same underlying stochastic process, the likelihood ratio statistics for POLSAR covariance matrix is considered:

$$Q = \frac{(L_x + L_y)^{d \cdot (L_x + L_y)}}{L_x^{d \cdot L_x} L_y^{d \cdot L_y}} \frac{|Z_x|^{L_x}|Z_y|^{L_y}}{|Z_x + Z_y|^{(L_x + L_y)}}$$

Taking the log-transformation of the above equation, and note that $C_{vx} = Z_x/L_x$, $C_{vy} = Z_y/L_y$ and $C_{vxy} = (Z_x + Z_y)/(L_x + L_y)$ then:

$$Q = \frac{|C_{vx}|^{L_x} \cdot |C_{vy}|^{L_y}}{|C_{vxy}|^{L_x + L_y}} \quad (9)$$

$$\ln Q = L_x \ln |C_{vx}| + L_y \ln |C_{vy}| - (L_x + L_y)\ln |C_{vxy}| \quad (10)$$

To detect changes, a test statistic is developed based on this measure of distance. This means a distribution is to be derived for the dissimilarity measure. However, in the original work [1], only an asymptotic distribution has been proposed.

III. SCALAR STATISTICAL MODELS FOR POLSAR

In this section, several scalar statistical models for POLSAR are presented. Section III-A briefly introduces the basic foundations, concepts and notation used in this paper, while section III-B presents the theoretical models together with mathematical evidence for two related points. The first point is that the POLSAR data is multiplicative and heteroskedastic in its original domain. And the second conclusion states that log-transformation converts it into an additive and homoskedastic model. Some consistent measures of distance are then derived and presented in section III-C.

A. Basics of POLSAR Statistical Analysis

In this paper, the POLSAR scattering vector is denoted as s. In the case of partial polarimetric SAR (single polarization in transmit and dual polarization in receipt), the vector is two-dimensional ($d = 2$) and is normally written as:

$$s_{part} = \begin{bmatrix} S_h \\ S_v \end{bmatrix} \qquad (11)$$

In the case of full and monostatic POLSAR data, the vector is three-dimensional ($d = 3$) and is presented as:

$$s_{full} = \begin{bmatrix} S_{hh} \\ \sqrt{2}S_{hv} \\ S_{vv} \end{bmatrix} \qquad (12)$$

Let $\Sigma = E[ss^{*T}]$ denote the population expected value of the POLSAR covariance matrix, where s^{*T} is the complex conjugate transpose of s. Assuming s is jointly circular complex Gaussian with the expected covariance matrix Σ, then the probability density function (PDF) of s can be written as:

$$pdf(s; \Sigma) = \frac{1}{\pi^d |\Sigma|} e^{-s^{*T}\Sigma^{-1}s} \qquad (13)$$

where $||$ denotes the matrix determinant.

The sample POLSAR covariance matrix is formed as the mean of Hermitian outer product of independent single-look scattering vectors,

$$C_v = \langle ss^{*T} \rangle = \frac{1}{L} \sum_{i=1}^{L} s_i s_i^{*T} \qquad (14)$$

where s_i denotes the single-look scattering vector, which equals s_{part} for the case of partial POLSAR or s_{full} for the case of full polarimetry, and L is the number of looks.

Complex Wishart distribution statistics are normally used for the scaled covariance matrix $Z = LC_v$, whose PDF is given as:

$$pdf(Z; d, \Sigma, L) = \frac{|Z|^{L-d}}{|\Sigma^L|\Gamma_d(L)} e^{-tr(\Sigma^{-1}Z)} \qquad (15)$$

with $\Gamma_d(L) = \pi^{d(d-1)/2} \prod_{i=0}^{d-1} \Gamma(L - i)$ and d is the dimensional number of the POLSAR covariance matrix.

The approach taken in this paper differs by applying the homoskedastic log transformation on a less-than-well-known result for the determinant of the covariance matrix. Goodman [14] proved that the ratio between the observable and expected values of the sample covariance matrix determinants behave like a product of d chi-squared random variables with different degrees of freedom:

$$\chi_L^d = (2L)^d \frac{|C_v|}{|\Sigma_v|} \sim \prod_{i=0}^{d-1} \chi^2(2L - 2i) \qquad (16)$$

Its log-transformed variable consequently behaves like a summation of d log-chi-squared random variables with the same degrees of freedom

$$\Lambda_L^d = ln\left[(2L)^d \frac{|C_v|}{|\Sigma_v|}\right] \sim \sum_{i=0}^{d-1} \Lambda^\chi(2L - 2i) \qquad (17)$$

with $\Lambda^\chi(k) \sim \ln\left[\chi^2(k)\right]$. We will now use this result to develop the statistical models for POLSAR.

B. Original Hetoroskedastic Domain and the Homoskedastic Log-Transformation

In this section the multiplicative nature of POLSAR data is first illustrated. Log-transformation is then applied to convert the data into a more familiar additive model. Heteroskedasticity, which is defined as the dependence of variance upon the underlying signal, is shown to be present in the original POLSAR data. In the log-transformed domain, a homoskedastic model is demonstrated, where sample variance is fixed and thus independent of the underlying signal. Several intermediate mathematical steps are not shown here, but can be found in Appendix A.

From Eqns. 16 and 17 we can deduce the following relationships:

$$|C_v| \quad \sim \quad |\Sigma_v| \cdot \frac{1}{(2L)^d} \cdot \prod_{i=0}^{d-1} \chi^2(2L - 2i) \qquad (18)$$

$$\ln|C_v| \quad \sim \quad \ln|\Sigma_v| - d \cdot \ln(2L) + \sum_{i=0}^{d-1} \Lambda(2L - 2i) \quad (19)$$

In a given homogeneous POLSAR area, the parameters Σ_v, d and L can be considered constant. Thus Eqn. 18 indicates that in the original POLSAR domain, a multiplicative speckle noise pattern is present. At the same time, Eqn. 19 shows that the logarithmic transformation has converted this to the more familiar additive noise.

Since chi-squared random variables $X \sim \chi^2(k)$ follow a known PDF:

$$pdf(x; 2L) = \frac{x^{L-1}e^{-x/2}}{2^L\Gamma(L)} \qquad (20)$$

applying the variable change theorem, its log-transformed variable follows the PDF of:

$$pdf(x; 2L = k) = \frac{e^{Lx - e^x/2}}{2^L\Gamma(L)} \qquad (21)$$

Using these PDFs, the characteristic functions (CF) of both the chi-squared and log-chi-squared random variables can be written as:

$$CF_\chi(t) \quad = \quad (1 - 2it)^L \qquad (22)$$

$$CF_\Lambda(t) \quad = \quad 2^{it}\frac{\Gamma(L + it)}{\Gamma(L)} \qquad (23)$$

Their means and variances can subsequently be computed from these characteristic functions, leading to the following relationships:

$$avg\,[\chi(2L)] \quad = \quad 2L \qquad (24)$$
$$var\,[\chi(2L)] \quad = \quad 4L \qquad (25)$$
$$avg\,[\Lambda(2L)] \quad = \quad \psi^0(L) + \ln 2 \qquad (26)$$
$$var\,[\Lambda(2L)] \quad = \quad \psi^1(L) \qquad (27)$$

where $\psi^0()$ and $\psi^1()$ represent the digamma and trigamma functions respectively.

Since the average and variance of both chi-squared distribution and log-chi-squared distribution are constant, the

product and summation of these random variables also has fixed summary statistics. Specifically:

$$avg\left[\prod_{i=0}^{d-1}\chi^2(2L-2i)\right] = 2^d \cdot \prod_{i=0}^{d-1}(L-i),$$

$$var\left[\prod_{i=0}^{d-1}\chi^2(2L-2i)\right] = \prod_{i=0}^{d-1}4(L-i)(L-i+1) - \prod_{i=0}^{d-1}4(L-i)^2,$$

$$avg\left[\sum_{i=0}^{d-1}\Lambda(2L-2i)\right] = d \cdot \ln 2 + \sum_{i=0}^{d-1}\psi^0(L-i),$$

$$var\left[\sum_{i=0}^{d-1}\Lambda(2L-2i)\right] = \sum_{i=0}^{d-1}\psi^1(L-i)$$

Combining these results with Eqns. 18 and 19, we have:

$$avg\left[|C_v|\right] = \frac{|\Sigma_v|}{L^d}\prod_{i=0}^{d-1}(L-i) \tag{28}$$

$$var\left[|C_v|\right] = \frac{|\Sigma_v|^2\left[\prod_{i=0}^{d-1}(L-i)(L-i+1) - \prod_{i=0}^{d-1}(L-i)^2\right]}{L^{2d}} \tag{29}$$

$$avg\left[\ln|C_v|\right] = \ln|\Sigma_v| - d \cdot \ln L + \sum_{i=0}^{d-1}\psi^0(L-i) \tag{30}$$

$$var\left[\ln|C_v|\right] = \sum_{i=0}^{d-1}\psi^1(L-i) \tag{31}$$

For a real world captured image, while the parameters d and L do not change for the whole image, the underlying Σ_v is expected to differ from one region to the next. Thus over a heterogeneous scene, the stochastic process for $|C_v|$ and $\ln|C_v|$ vary depending on the underlying signal Σ_v. In such context, Eqn. 29 implies that the variance of $|C_v|$ also differs depending on the underlying signal Σ_v (i.e. it is heteroskedastic). At the same time, in the log-transformed domain, Eqn. 31 reveals that the variance of $\ln|C_v|$ is invariant and independent of Σ_v (i.e. it is homoskedastic).

C. Consistent Measures of Distance for POLSAR

Similar to the way dispersion and contrast is defined for one-dimensional SAR [15], this section introduces the consistent sense of distance for POLSAR. Assuming, on the one hand, that the true value of the underlying signal Σ_v is known *a priori*, then the random variables, ratio ($\mathbb{R}$) and log-distance ($\mathbb{L}$) are observable according to the following definitions:

$$\mathbb{R} = \frac{|C_v|}{|\Sigma_v|} \tag{32}$$

$$\mathbb{L} = \ln|C_v| - \ln|\Sigma_v| \tag{33}$$

On the other hand, under a looser assumption where the POLSAR data is known to have come from a homogeneous area, but the true value of the underlying signal Σ_v is *unknown*, the dispersion ($\mathbb{D}$) and contrast ($\mathbb{C}$) random variables are the observables defined as:

$$\mathbb{D} = \ln|C_v| - avg(\ln|C_v|) \tag{34}$$

$$\mathbb{C} = \ln(|C_{v1}|) - \ln(|C_{v2}|) \tag{35}$$

Using the results from Eqns. 18, 19 and 30 we have

$$\mathbb{R} \sim \frac{1}{(2L)^d} \cdot \prod_{i=0}^{d-1}\chi^2(2L-2i) \tag{36}$$

$$\mathbb{L} \sim \sum_{i=0}^{d-1}\Lambda(2L-2i) - d \cdot \ln(2L) \tag{37}$$

$$\mathbb{D} \sim \sum_{i=0}^{d-1}\Lambda(2L-2i) - d \cdot \ln 2 + k \tag{38}$$

$$\mathbb{C} \sim \sum_{i=0}^{d-1}\Delta(2L-2i) \tag{39}$$

with $\Delta(2L) \sim \Lambda(2L) - \Lambda(2L)$ and $k = \sum_{i=0}^{d-1}\psi^0(L-i)$

Thus the characteristic functions for the summative random variables is derived in Appendix B as:

$$CF_{\Lambda_L^d}(t) = \frac{2^{idt}}{\Gamma(L)^d}\prod_{j=0}^{d-1}\Gamma(L-j+it) \tag{40}$$

$$CF_{\mathbb{L}}(t) = \frac{1}{L^{idt}\Gamma(L)^d}\prod_{j=0}^{d-1}\Gamma(L-j+it) \tag{41}$$

$$CF_{\mathbb{D}}(t) = \frac{e^{ikt}}{\Gamma(L)^d}\prod_{j=0}^{d-1}\Gamma(L-j+it) \tag{42}$$

$$CF_{\Delta(2L)} = \frac{\Gamma(2L)B(L-it,L+it)}{\Gamma(L)^2} \tag{43}$$

$$CF_{\mathbb{C}}(t) = \prod_{j=0}^{d-1}\frac{\Gamma(2L-2j)B(L-j-it,L-j+it)}{\Gamma(L-j)^2} \tag{44}$$

Since each elementary component follows fixed distributions (i.e. $\chi^2(2L), \Lambda(2L), ...$), it is natural that these variables also follow fixed distributions. Moreover, note that they are independent of the underlying signal Σ_v.

IV. SAR AS A ONE-DIMENSIONAL CASE OF POLSAR

The previous section introduced theoretical models for 3-dimensional ($d = 3$) full polarimetric and 2-dimensional ($d = 2$) partial polarimetry, cases. This section will show that the model is equally applicable to the 1-dimensional ($d = 1$) case, which is physically equivalent to collapsing the multi-dimensional POLSAR dataset into conventional single dimensional SAR data. Mathematically, the sample covariance matrix is reduced to the sample variance while the determinant is equivalent to the scalar value. As variance is equal to intensity for SAR data, our result is consistent with previous results for SAR intensity data. Hence this derivation can be considered as cross-validation evidence for the proposed POLSAR models as well as reminding us that SAR is a special case of POLSAR.

The results for our models can be summarized using the

following equations:

$$\mathbb{R} = \frac{|C_v|}{|\Sigma_v|} \sim \frac{1}{(2L)^d} \prod_{i=0}^{d-1} \chi^2(2L-2i) \tag{45}$$

$$\mathbb{L} = \ln|C_v| - \ln|\Sigma_v| \sim \sum_{i=0}^{d-1} \Lambda(2L-2i) - d \cdot \ln 2L \tag{46}$$

$$\mathbb{D} = \ln|C_v| - avg(\ln|C_v|) \sim \sum_{i=0}^{d-1} \Lambda(2L-2i) - d\ln 2 + k \tag{47}$$

$$\mathbb{C} = \ln|C_{1v}| - \ln|C_{2v}| \sim \sum_{i=0}^{d-1} \Delta(2L-2i) \tag{48}$$

$$\mathbb{A} = avg(\mathbb{L}) = \sum_{i=0}^{d-1} \psi^0(L-i) - d \cdot \ln L \tag{49}$$

$$\mathbb{V} = var(\mathbb{L}) = \sum_{i=0}^{d-1} \psi^1(L-i) \tag{50}$$

$$\mathbb{E} = mse(\mathbb{L}) = \left[\sum_{i=0}^{d-1} \psi^0(L-i) - d \cdot \ln L\right]^2 + \sum_{i=0}^{d-1} \psi^1(L-i) \tag{51}$$

Upon setting $d = 1$ into the above equations, Appendix C shows that the reduced results are consistent with the following two cases. First is the following results obtained from our previous work on single-look SAR [15] , i.e. $d = L = 1$,

$$I \sim \bar{I} \cdot pdf\left[e^{-R}\right]$$

$$\log_2 I \sim \log_2 \bar{I} + pdf\left[2^x e^{-2^x} \ln 2\right]$$

$$\mathbb{R} = \frac{I}{\bar{I}} \sim pdf\left[e^{-x}\right]$$

$$\mathbb{L} = \log_2 I - \log_2 \bar{I} \sim pdf\left[2^x e^{-2^x} \ln 2\right]$$

$$\mathbb{D} = \log_2 I - avg(\log_2 I) \sim pdf\left[e^{-(2^x e^{-\gamma})} 2^x e^{-\gamma} \ln 2\right]$$

$$\mathbb{C} = \log_2 I_1 - \log_2 I_2 \sim pdf\left[\frac{2^x}{(1+2^x)^2} \ln 2\right]$$

$$\mathbb{A} = avg(\mathbb{L}) = -\gamma/\ln 2$$

$$\mathbb{V} = var(\mathbb{L}) = \frac{\pi^2}{6} \frac{1}{\ln^2 2}$$

$$\mathbb{E} = mse(\mathbb{L}) = \frac{1}{\ln^2 2}(\gamma^2 + \pi^2/6) = 4.1161$$

The second is the following well-known results for multi-look SAR, i.e. $d = 1, L > 1$:

$$I \quad \sim \quad pdf\left[\frac{L^L x^{L-1} e^{-Lx/\bar{I}}}{\Gamma(L)\bar{I}^L}\right] \tag{52}$$

$$N = \ln I \quad \sim \quad pdf\left[\frac{L^L}{\Gamma(L)} e^{L(x-\bar{N})-Le^{x-\bar{N}}}\right] \tag{53}$$

Furthermore, the following derivations for multi-look SAR data show that it can be considered either as extensions of the corresponding single-look SAR results or as simpler case

of the POLSAR results:

$$\mathbb{R} = \frac{I}{\bar{I}} \sim pdf\left[\frac{L^L x^{L-1} e^{-Lx}}{\Gamma(L)}\right]$$

$$\mathbb{L} = \ln I - \ln \bar{I} \sim pdf\left[\frac{L^L e^{Lt-Le^t}}{\Gamma(L)}\right]$$

$$\mathbb{D} = \ln I - avg(\ln I) \sim pdf\left[\frac{e^{L[x-\psi^0(L)]-e^{[x-\psi^0(L)]}}}{\Gamma(L)}\right]$$

$$\mathbb{C} = \ln I_1 - \ln I_2 \sim pdf\left[\frac{e^x}{(1+e^x)^2}\right]$$

$$\mathbb{A} = avg(\mathbb{L}) = \psi^0(L) - \ln L$$

$$\mathbb{V} = var(\mathbb{L}) = \psi^1(L)$$

$$\mathbb{E} = mse(\mathbb{L}) = \left[\psi^0(L) - \ln L\right]^2 + \psi^1(L)$$

V. VALIDATING THE PROPOSED MODELS AGAINST REAL-LIFE DATA

This section aims to verify the theoretical models against practical data. Since it is shown that the model for the case of $d = 1$ matches exactly with the traditional model for SAR intensity, which have been validated extensively, only a simple validation is presented for this case.

Fig. 1 presents the results of an experiment carried out for the stated purpose. In the experiment, the intensity of single-channel SAR data (HH) for a homogeneous area in the AIRSAR Flevoland dataset is extracted. The histograms for the log-distance and contrast are then plotted against the theoretical PDF given above. The plot is obtained with ENL set to the nominal number of 4, and a good visual match is apparent, providing us a simple validation of the result.

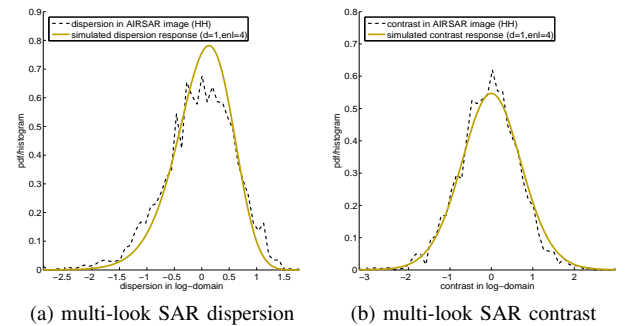(a) multi-look SAR dispersion   (b) multi-look SAR contrast

Fig. 1: Multi-Look SAR dispersion and contrast: modelled response matches very well with real-life captured data. It should be noted that an even better match than what is shown here is presented in Fig. 7 where a better ENL estimation is employed.

The remainder of this section now focuses on validating the models for both partial ($d = 2$) and full ($d = 3$) POLSAR. Specifically, subsection V-A demonstrates a naive validation, where the nominal ENL is used for the model. While the match appears to be reasonably good, it can be further improved. Subsection V-B discusses why the nominal look-number given by (POL)SAR processors may not be accurate, while subsection V-C proposes a new technique in

estimating the Effective Number of Looks (ENL) using the consistent variance found in a homoskedastic model. With the newly estimated ENL, subsection V-D demonstrates that the match between the theoretical model and the practical data is indeed further improved.

A. Using the nominal ENL to validate the theoretical models

The stochastic models derived in the previous sections can be visualised using histograms of the simulated data. Their accuracy can be verified by comparing to histograms from real-life data samples extracted over a homogeneous area.

For this purpose, a homogeneous sample area was chosen from the AIRSAR Flevoland POLSAR data. Both the determinant and the log-transformed models are to be validated together with the associated dissimilarity measures, namely the determinant ratio, log-distance, dispersion and contrast. These are closely related in that the determinant and determinant ratio are simply scaled versions of each other. Meanwhile, the log-determinant, log-distance and dispersion are simply shifted versions of each other. Nevertheless, all will be separately evaluated in this experiment in order to reveal an interesting phenomenon.

The least-assumed stochastic processes for dispersion and contrast are validated first. For each pixel in the region, the determinant of the covariance matrix is computed and the log-transformation applied. Then the average log-determinant of the POLSAR covariance matrix, i.e. $avg(ln|C_v|)$, is measured for dispersion. Subsequently the observable samples of dispersion and contrast are computed according to Eqns. 34 and 35 in order to plot their histograms.

At the same time, theoretical simulations according to Eqns. 38 and 39 are carried out. Here a nominal look-number L=4 is used while the dimensional number is set to either 3 or 2 for a full or partial polarimetric SAR dataset respectively. The plots, presented in Fig. 2 show a good visual match between the model and real data, validating the theoretical models for dispersion and contrast.

Apart from dispersion and contrast, the other four models to be verified require an estimation of the "ground truth" underlying signal $|\Sigma_v|$. There are two ways to estimate this quantity over an homogeneous area. The traditional way is to simply set the ground truth signal equal to the average of the POLSAR covariance matrix in its original domain, i.e. $\Sigma_v = avg(C_v)$. Another approach is to estimate the true signal from the average of the log-determinant of the POLSAR covariance matrix (i.e. $avg[ln|C_v|]$) using Eqn. 30. Both approaches will be presented in this section. As the log-determinant average has already been computed, the second approach is hence used first for the validation of determinant-ratio and log-distance.

Fig. 3 plots the determinant-ratio and log-distance models against real-life data. In this experiment, the theoretical models are simulated using Eqns 36 and 37, while the observable samples are computed using Eqns 32 and 33 with the true signal estimated from the log-determinant average, i.e. $avg(ln|C_v|)$. A close match is again observed, validating the models for log-distance and determinant ratio.
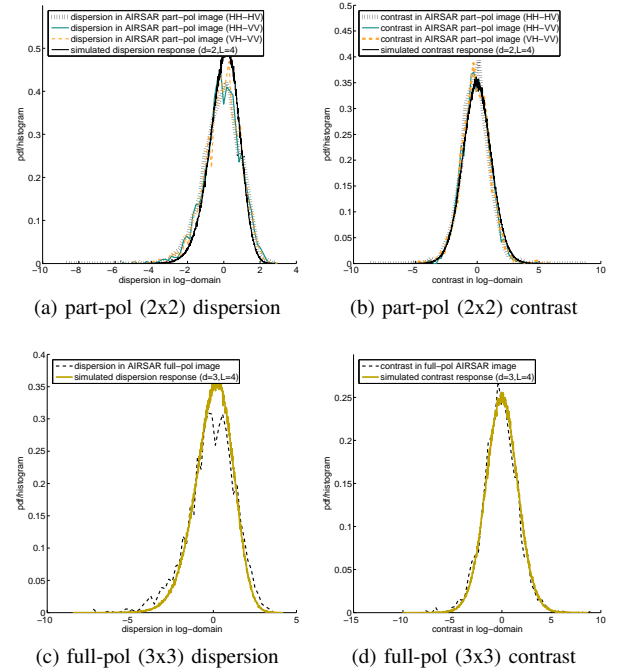

Fig. 2: Validating the dispersion and contrast models against both partial and full polarimetric AIRSAR Flevoland data.
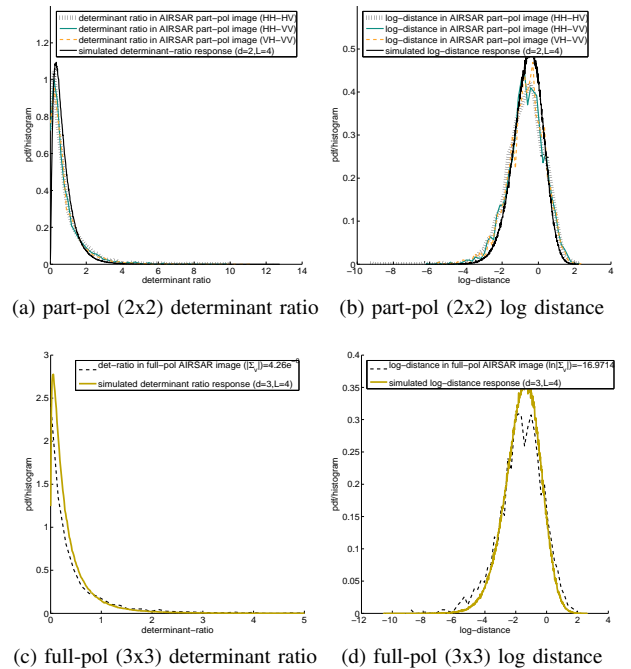
(a) part-pol (2x2) dispersion

(b) part-pol (2x2) contrast

(c) full-pol (3x3) dispersion

(d) full-pol (3x3) contrast

Fig. 3: Validating determinant-ratio and log-distance models with $|\Sigma_v|$ is computed using $avg(ln|C_v|)$

(a) part-pol (2x2) determinant ratio

(b) part-pol (2x2) log distance

(c) full-pol (3x3) determinant ratio

(d) full-pol (3x3) log distance

Since the models for the determinant and log-determinant are just scaled or shifted versions of the models for determinant-ratio and log-distance, similar validation results are to be expected. However, an interesting phenomena is observed during the validation process for the determinant and its log-transformed model, where the theoretical behaviour is

simulated by Eqns. 18 and 19. The phenomena occurs when the true signal is estimated using the average of the sample covariance matrix in its original domain. Subsequently in the validation plots presented in Fig 4, some small translation and scaling discrepancies are observed.
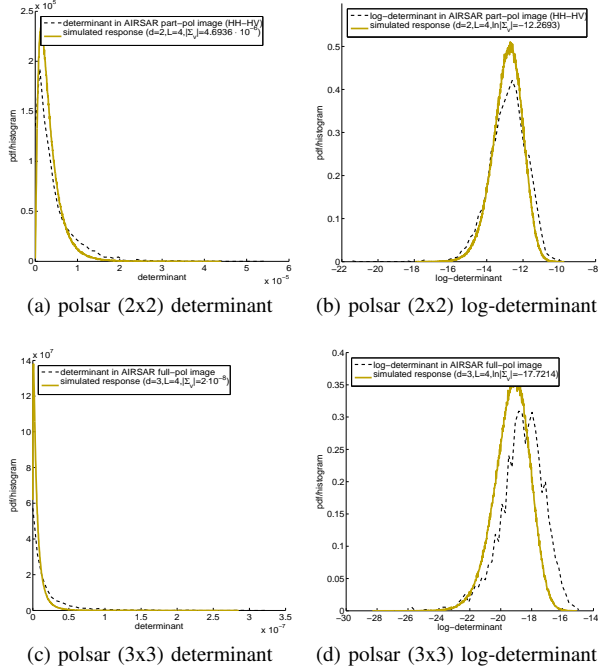

(a) polsar (2x2) determinant (b) polsar (2x2) log-determinant

(c) polsar (3x3) determinant (d) polsar (3x3) log-determinant

Fig. 4: Validating determinant and log-determinant models with $\Sigma_v = avg(C_v)$

In summary the dispersion and contrast measures of distance are shown to match reasonably well with the practical data. The same can be stated for the other four models, namely: determinant, log-determinant, determinant ratio and log-distance, if the underlying parameters can be estimated reasonably well for the given image. However as described above a single "true signal" $|\Sigma_v|$ can have two different estimated values, depending on which estimation method was being used. The discrepancy between these two values suggests that at least one parameter for the models was inaccurately estimated. This is discussed in the next subsection.

B. Difference between the theoretical assumptions and the conditions found in practice

Even though the assumptions made in developing this theory have intentionally been kept minimal, in common with other similar derivations the proposed model in this paper is built upon certain presumptions. However, practical conditions may not always satisfy these prerequisites, a common and observable gap is noticed between the conditions found in practical real-life data and the theoretical assumptions.

The assumption of statistical independence between samples (for both SAR and POLSAR data) is reasonable given that the transmission and receipt of analogue signals is independent for each radar pulse, i.e. for each resolution cell. However, the actual imaging mechanism in a real-life (POL)SAR processor

is of a digital nature, where the analogue signal is fed into an analogue-to-digital (ADC) sampling and conversion process. Theoretically it is possible to define a sampling rate so that each digital pixel corresponds exactly to an separate analogue physical cell. Practically however, to ensure "perfect reconstruction", the sampling rate is normally set at a slightly higher value than the Nyquist rate.

Thus in practical images, each physical radar cell may be spread over more than a single pixel, resulting in both a higher correlation between neighbouring pixels [16] and a reduced effective number of look [4] [17]. The over-sampling practice is also documented by the producers of SAR processors. For AIRSAR, the sampling rate and pulse bandwidth combinations are either 90/40MHz or 45/20MHz [18]. While for RadarSat2, the pixel resolution and range - azimuth resolution combination for SLC fine-quad mode is advertised as $(4.7 \cdot 5.1)m^2/(5.2 \cdot 7.7)m^2$ [19]. In short, while the independent sample assumption is made out of necessity in theory, due to over-sampling practice in capturing systems, significant correlation is routinely observed among neighbouring samples. This documented imperfection also leads to the rise of effective number-of-look concept (ENL), which is almost always smaller than the nominal look-number.

The proposed model apparently can handle this imperfection. The handling process, however, is slightly more complex. Instead of adopting the nominal Number of Looks given by the SAR processor, an ENL must first be estimated from the given data. This is discussed in the next subsection.

C. ENL Estimation for POLSAR data

The common approach in ENL estimation is to investigate the summary statistics of a known homogeneous area in the given data before making inferences about the inherent ENL. The summary statistics for $|C_v|$ and $\ln|C_v|$ have been derived in Section III-B, where Eqn. 30 indicates that there is a relationship among $|avg(C_v)|, avg(\ln|C_v|), d, L$. In a given POLSAR dataset, since all values of $|avg(C_v)|, avg(\ln|C_v|), d$ are known, it is possible to estimate the "effective" number of looks, by finding an L that ensures the above relationship is valid. This approach was taken in [17], where an equation of exactly the same form as Eqn. 30 was used to estimate the ENL. However, the only known way to solve the equation for unknown L requires the use of an "iterative numerical method".

This paper instead proposes an alternative approach that makes use of variance statistics in the homoskedastic log-domain. Specifically, Eqn. 31 can be rewritten as:

$$var\left[ln|C_v|\right] = f(L) = \sum_{i=0}^{d-1} \psi^1(L-i) \qquad (54)$$

where $\psi^1()$ again denotes the tri-gamma function.

Thus theoretically, given some measurable value for $var\left[ln|C_v|\right]$, one could solve the above equation for unknown L, although it would also require some iterative computation. Practically however, the shape of the right-hand-side can be pre-computed and for each computed value of $var\left[ln|C_v|\right]$, a corresponding value for L can be found by referencing

the variance value on the pre-computed graph, or from the following equation:

$$\hat{L} = d\left(\frac{1}{var(\ln|C_v|)} + 0.5\right) \tag{55}$$

Fig. 5 shows the shapes of the function defined in Eqn. 54 for SAR and partial-POLSAR data $f_{d=1}(L)$ and $f_{d=2}(L)$ as well as illustrating the simplified approximation formula (Eqn. 55).
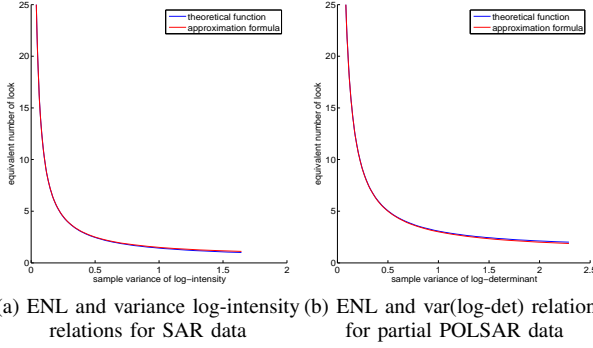

(a) ENL and variance log-intensity relations for SAR data

(b) ENL and var(log-det) relations for partial POLSAR data

Fig. 5: The relation between ENL and sample variance for log-determinant/log-intensity plots.

D. Using estimated ENL to better explain practical data

To demonstrate the improvement obtained using this ENL estimation, a single-look complex fine-quad RADARSAT2 dataset is used as illustration. Nine-look processing is first applied, followed by calculation of the dispersion histogram in the log-transformed domain for an homogeneous area. The histograms for both one-dimensional SAR and two-dimensional partial POLSAR data are plotted in Fig. 6 against the theoretical models for the nominal ENL value of 9. As expected the match is evidently not very close.

We now compare this to the estimated ENL approach. First, an ENL estimate is obtained from the observable variance of the log-determinant. Then the new sample histogram is overlaid on the same figure, showing a much better consistency. This procedure can always be carried out for a given dataset, as long as a homogeneous area can be defined and extracted.

The same approach can be applied on the AIRSAR Flevoland data to improve the validation described earlier. Fig. 7 shows that the over-sampling issue is also present in the AIRSAR Flevoland dataset, even though it is to a much lesser extent. Still, the "corrected" ENL offers an evidently better match between the model and real-life data.

VI. DISCUSSION

Let us begin by noting a few theoretical properties of the proposed statistical models. First, the use of covariance matrix log-determinant may be related to the standard eigen-decomposition method of the POLSAR covariance matrices. In fact, the log-determinant can also be computed as the sum of log-eigenvalues. Specifically $\ln|M| = \sum \ln \lambda_M$ where λ_M denotes all the eigenvalues of M. Thus similar to other eigenvalue based approach (e.g. entropy/anisotropy, ...), the

(a) Handling over-sampling practice in Radarsat2 one-dimensional SAR data (HH)

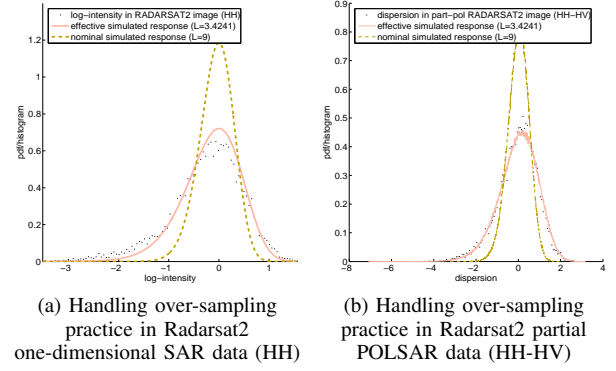(b) Handling over-sampling practice in Radarsat2 partial POLSAR data (HH-HV)

Fig. 6: Nine-look processed Radarsat2 data does not always exhibit nine-look data characteristics. However the homoskedastic model in the log-transformed domain can successfully estimate an effective ENL which matches the data much more closely.

(a) Handling over-sampling practice in AIRSAR part-pol dataset

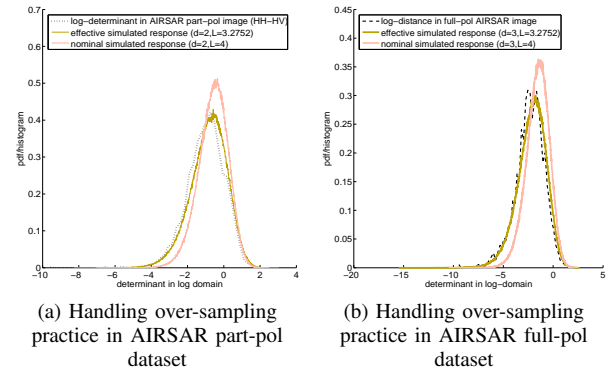(b) Handling over-sampling practice in AIRSAR full-pol dataset

Fig. 7: AIRSAR Flevoland also exhibits phenomena of over-sampling practice, through to a lesser extent than the RADARSAT2 data.

models presented here are invariant to polarization basis transformations.

Second, the models are developed for the POLSAR covariance matrix. However, since the POLSAR coherency matrix is related to the covariance matrix via a unitary transformation which preserves the determinant, the model should also be applicable to the coherency matrix.

It should be noted that the models are far from complete. While it is desirable to reduce the multi-dimensonal POLSAR data to a scalar value for many applications, such a reduction is unlikely to be lossless. Thus the use of this technique could be complemented with some high-dimensional POLSAR target-decomposition techniques, such as the Freeman Durden decomposition [20] or the entropy/anisotropy decomposition [21] or similar.

Nevertheless the proposed models are promising. Even though initially developed for partial and monostatic POLSAR data, it was shown to be applicable to traditional SAR data as well. Since the models assumptions are quite minimal, they may potentially applicable to bi-static and interferometric data, although that would require further study.

Intuitively, the concept of the determinant being representative of the POLSAR data can be thought of as being similar to the concept of using the magnitude as being representative of a complex number (in a sense this is also why intensity is widely considered representative of the SAR data complex). Similar to the determinant, the magnitude observable is also scalar and is not lossless. To fully represent the complex number, another observable is needed besides the magnitude. The magnitude however is much more widely used, as it can be shown that its is invariant to a change in the reference frame. Similarly, the determinant of the POLSAR covariance matrix is also scalar and invariant to a change of polarization basis. Thus while it is not fully representative of the POLSAR data, it can be said to be highly representative of it. The important thing is that, it can be used to give a scalar comparison of the multi-dimensional data. This is also similar to the standard use of the magnitude when two or more complex numbers are to be compared.

This leads to the application of the models in deriving discrimination measures. Besides the above properties, the theoretical models may also provide an alternative derivation for the widely used likelihood test statistics in POLSAR. In view of the models given in Eqns 18 & 19, the likelihood test statistics exposed in [1] and rewritten in Eqns 9 & 10 can be simulated as:

$$\ln Q \sim k + L_x \Lambda_{L_x}^d + L_y \Lambda_{L_y}^d - (L_x + L_y)\Lambda_{(L_x+L_y)}^d$$

$$Q \sim e^k \frac{(\chi_{L_x}^d)^{L_x} \cdot (\chi_{L_y}^d)^{L_y}}{(\chi_{L_x+L_y}^d)^{L_x+L_y}}$$

where $k = d\left[(L_x + L_y)\ln(L_x + L_y) - L_x \ln L_x - L_y \ln L_y\right]$. As a by-product of this exact derivation, the current paper also proposed several simpler discrimination measures for the common case of $L_x = L_y$.

Similar to the way that other measures of distance can be used to derive POLSAR classifiers [8], change detectors [1], edge detectors [22] or other clustering and speckle filtering techniques [15] [23], new detection, classification, clustering or speckle filtering algorithms can be derived using the models presented in this paper. These applications however are not included in this paper, but rather left as a suggestion for future investigations. There are a few reasons for this decision. The first is that the advantages of the proposed models have been demonstrated through a few applications in this paper: the first being a faster ENL evaluation for POLSAR data and the second being the visual evaluation of POLSAR speckle filters. The second reason is that such an application would be quite big in scope, and as such would easily distract the reader from the main proposal of this paper. Last but not least, this paper focuses on the proposal of several scalar and representative statistical models for POLSAR, which results in associated statistical models and discrimination measures. It does not, technically speaking, focuses on proposing new discrimination measures.

The advantages of this proposal are thus to be compared against other published models for POLSAR. Consequently, the methodology to evaluate the result of this proposal is a bit unusual. While quantitative evaluation is normally employed, in this theoretical model proposal only qualitative evaluation are shown. This is because compared to existing published observables for POLSAR, the advantage of the proposed observables are qualitative which does not requires numerical quantitative comparisons. Instead a straightforward binary evaluation would be sufficient. In comparison to other scalar models for POLSAR, the proposed models for determinant and its log-transformed version are representative are highly representative of the POLSAR data. This is because these models collapses into the representative SAR intensity when the multi-dimensional data is collapsed into the traditional one-dimensional SAR data. This is proven in section IV. No other existing models for POLSAR is known to have this property.

Other advantage is that compared to other proposed scalar models for POLSAR, only these proposed statistical models lead to existing discrimination measures. This argument is supported by an extensive literature survey in section II. There not only existing published scalar models for POLSAR are reviewed to show that none of them lead to discrimination measure, existing discrimination measures for POLSAR are also extensively surveyed leaving virtually no chance of there exists an existing scalar statistical model for POLSAR which leads to existing discrimination measures.

There may have many beneficials implications for this proposal. One of the main benefits is believed to be that: this proposal allows the extension of many of existing SAR data processing technique toward POLSAR. This is illustrated through an example which extends the SAR speckle filters evaluation technique towards POLSAR. In evaluating SAR speckle filters, the intensity ratio is widely used. Specifically, in its original multiplicative domain, the ratio of the filtered output and the noisy input image represents the noise being removed. Assuming a perfect filtering condition, the ratio image should only contain random noise. Thus a commonly used visual evaluation is to simply plot the ratio image and determine if any image features have also been removed.

Since the POLSAR determinant ratio has been shown to be equivalent to the SAR intensity ratio, this technique can be equally applied to evaluate POLSAR speckle filters. In fact better results can be achieved. In [24], it has been shown that the multiplicative ratio is not well suited to digital image presentation, which is linear and additive in nature. Thus logarithmic transformation can be applied to convert the multiplicative determinant-ratio into the linear subtractive contrast.

To demonstrate this feature, the technique is used to evaluate the performance of 3×3 and 5×5 boxcar POLSAR filters on the AIRSAR Flevoland partial polarimetric data (HH-HV). A square 700×700 pixel patch is first extracted from the AIRSAR dataset, and the two POLSAR speckle filters are then applied to the patch. [1] The log-determinant images of the filtered outputs are displayed in Fig. 8. At the same time, the residual is computed for both filters, and the images are

---

[1] While the boxcar filters may not stay in the frontier of POLSAR speckle filtering, they are workable here since the focus of this experiment is not on finding the best POLSAR speckle filters available. Rather its purpose is to show a quick example of how an existing technique in SAR data processing can be easily adapted for POLSAR data.

also displayed in the same figure.

(a) Log-determinant Image of boxcar 3×3 speckle filter

(b) Log-determinant Image of boxcar 5×5 speckle filter

(c) Image of Log-determinant Residual for 3×3 filter
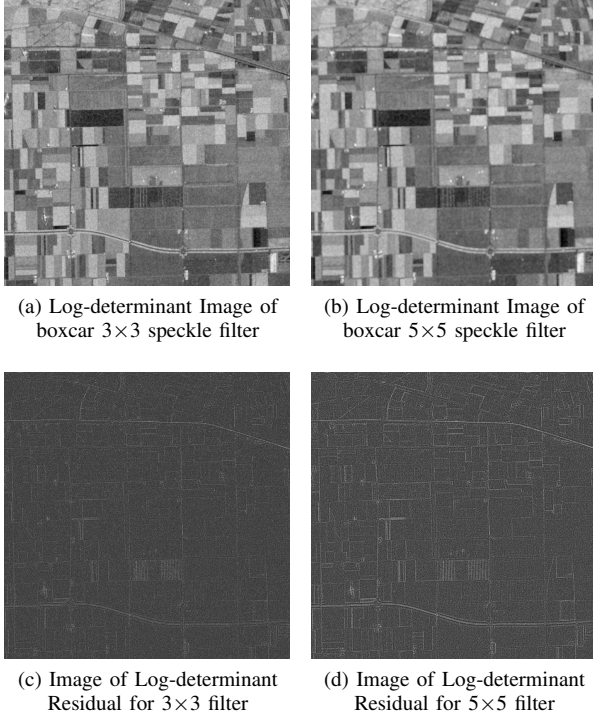
(d) Image of Log-determinant Residual for 5×5 filter

Fig. 8: Visually Evaluating POLSAR Boxcar 3×3 vs. 5×5 Speckle Filters on AIRSA Flevoland part-pol data (HH-HV).

Fig. 8 shows that not only does the log-determinant image offer a nice visualization of the scene, the distortion impact of the filter can also be made visible by the residual image. In this visual evaluation, while it is quite hard to observe the worsen blurring-effects of the boxcar 5×5 speckle filter compared to the 3×3 filter in the additive log-determinant image of the filtered output, such an observation can be made relatively easier by inspecting the residual image.

There are many similar SAR data processing technique that may be adaptable to POLSAR. Examples in the same topic of evaluating speckle filters include the use of the mean and variance of the ratio image, or ENL evaluation to quantitatively evaluate POLSAR speckle filters. Other topics that may also be connected include: speckle filtering, target detection, surface cover classification, edge detection ... and so on.

Currently while the field of SAR is much more developed than the field of POLSAR, the two fields however are quite separated. Hence many techniques applicable to SAR are not directly applicable to POLSAR. Under this context, the current proposal provide the bridge between these two separated fields, inviting potential extension of various SAR processing techniques to POLSAR data. For instance the earlier example illustrate that while intensity ratio was commonly used to carry out visually evaluation of SAR speckle filters, the newly proposed determinant ratio and its log-transformed version (i.e. contrast) are shown capable of visually evaluating POLSAR speckle filters. We believe there are many more unexplored possibilities for such applications.

VII. CONCLUSION

A number of scalar statistical models for the determinant of the POLSAR covariance matrix are proposed and validated in this paper, resulting in several consistent discrimination measures useful POLSAR applications. The theoretical models are shown to be comprehensive in that not only can they provide alternative and simple explanations to a range of theoretical concepts such as POLSAR test statistics or ENL estimation, but they can also be considered multi-dimensional extensions of traditional models for one-dimensional SAR data. The models are also practically useful since they provide several consistent discrimination measures. Moreover, compared to other scalar statistical models for POLSAR, the proposed models are excellent representations of the multi-dimensional POLSAR data. Consequently, the derived discrimination measures may be employed in a wide range of applications where a scalar number is required to represent the complex multi-dimensional POLSAR data. Thus the models are envisioned to form a bridge inviting the adaptation of many existing SAR data processing techniques for POLSAR data.

APPENDIX A
HOMOSKEDASTIC MODEL FOR THE LOG-DETERMINANT

A. Log-Chi-Square Distribution and its Derivatives

This section provides the mathematical derivations for the log-transformed version of chi-squared random variables.

Chi-squared random variables $\chi \sim \chi^2(k)$ follows the pdf:

$$pdf(\chi; k) = \frac{\chi^{(k/2)-1}e^{-\chi/2}}{2^{k/2}\Gamma\left(\frac{k}{2}\right)} \qquad (A.1)$$

Setting L=k/2 into Eqn. A.1

$$pdf(\chi) = \frac{\chi^{L-1}e^{-\chi/2}}{2^L\Gamma(L)} \qquad (A.2)$$

Applying the variable change theorem, which states that: if $y = \phi(x)$ with $\phi(c) = a$ and $\phi(d) = b$, then:

$$\int_a^b f(y)\,dy = \int_c^d f[\phi(x)]\frac{d\phi}{dx}dx \qquad (A.3)$$

into the log-transformation, which changes the random variables $\Lambda = ln(\chi)$, we have:

$$d\chi = e^\Lambda d\Lambda$$
$$\frac{\chi^{L-1}e^{-\chi/2}}{2^L\Gamma(L)}d\chi = \frac{(e^\Lambda)^{L-1}e^{-e^\Lambda/2}}{2^L\Gamma(L)}e^\Lambda d\Lambda$$

In other words, we have:

$$pdf(\Lambda; L) = \frac{e^{L\Lambda-e^\Lambda/2}}{2^L\Gamma(L)} \qquad (A.4)$$

From the PDF given in Eqn. A.4, a characteristic function can be computed. By definition, the characteristic function (CF) $\varphi_X(t)$ for a random variable X is computed as:

$$\varphi_X(t) = E\left[e^{itX}\right] = \int_{-\infty}^{\infty} e^{itx}\,dF_X(x)$$
$$= \int_{-\infty}^{\infty} e^{itx}f_X(x)\,dx$$

with $\varphi_x(t)$ is the characteristic function, $F_X(x)$ is the CDF function of X and $f_X(x)$ is the PDF function of X. Thus the characteristic function for the log-chi-squared distribution is defined as:

$$\varphi_\Lambda(t) = \int_0^\infty e^{itx} \frac{e^{Lx-e^x/2}}{2^L\Gamma(L)}\, dx \qquad (A.5)$$

The Gamma function is defined over the complex domain as: $\Gamma(z) = \int_0^\infty e^{-x}x^{z-1}dx$. Thus $\Gamma(L+it) = \int_0^\infty e^{-x}x^{L+it-1}dx$. Set $x = e^z/2$ then $dx = e^z/2dz$, we have $\Gamma(L+it) = \int_0^\infty e^{itz}\frac{e^{Lz-e^z/2}}{2^{L+it}}dz$

That is:

$$\varphi_\Lambda(t) = 2^{it}\frac{\Gamma(L+it)}{\Gamma(L)} \qquad (A.6)$$

Consequently, the first and second derivative of the log-chi-squared distribution can be computed. The first derivative is given as:

$$\frac{\partial\varphi_\Lambda(t)}{\partial t} = \frac{i2^{it}\Gamma(L+it)}{\Gamma(L)}\left[\ln 2 + \psi^0(L+it)\right] \qquad (A.7)$$

due to

$$\frac{\partial\Gamma(x)}{\partial x} = \Gamma(x)\psi^0(x),$$
$$\frac{\partial\Gamma(L+it)}{\partial t} = i\Gamma(L+it)\psi^0(L+it),$$
$$\frac{\partial 2^{it}}{\partial t} = i2^{it}\ln(2),$$
$$\partial(u \cdot v)/\partial t = u \cdot \partial v/\partial t + v \cdot \partial u/\partial t,$$

where $\psi^0()$ denotes the di-gamma function.

Meanwhile, the second derivative can be written as:

$$\frac{\partial^2\varphi_\Lambda(t)}{\partial t^2} = \frac{i^2 2^{it}\Gamma(L+it)}{\Gamma(L)}\left(\left[\ln 2 + \psi^0(L+it)\right]^2 + \psi^1(L+it)\right) \qquad (A.8)$$

due to:

$$\frac{d2^{it}\Gamma(L+it)}{dt} = i2^{it}\Gamma(L+it)\left[\ln 2 + \psi^0(L+it)\right],$$
$$\frac{d\psi^0(t)}{dt} = \psi^1(t),$$
$$\frac{d\psi^0(L+it)}{dt} = i\psi^1(L+it),$$
$$\partial(u \cdot v)/\partial t = u \cdot \partial v/\partial t + v \cdot \partial u/\partial t,$$

with $\psi^1()$ denotes the tri-gamma function.

The nth moments of random variable X can be computed from the derivatives of its characteristic function as:

$$E(\Lambda^n) = i^{-n}\varphi_\Lambda^{(n)}(0) = i^{-n}\left[\frac{d^n}{dt^n}\varphi_\Lambda(t)\right]_{t=0} \qquad (A.9)$$

Thus

$$E(\Lambda) = i^{-1}\left[\frac{d\varphi_\Lambda(t)}{dt}\right]_{t=0}$$
$$= i^{-1}\left[\frac{i2^{it}\Gamma(L+it)}{\Gamma(L)}\left[\ln 2 + \psi^0(L+it)\right]\right]_{t=0}$$

That gives the result:

$$avg(\Lambda) = \psi^0(L) + ln(2) \qquad (A.10)$$

Similarly, for the second moment,

$$E(\Lambda^2) = i^{-2}\left[\frac{d^2\varphi_\Lambda(t)}{dt^2}\right]_{t=0}$$
$$= \left[\frac{2^{it}\Gamma(L+it)}{\Gamma(L)}\left(\left[\ln 2 + \psi^0(L+it)\right]^2 + \psi^1(L+it)\right)\right]_{t=0}$$

That is equivalent to saying that

$$E(\Lambda^2) = \left[\psi^0(L) + \ln(2)\right]^2 + \psi^1(L) \qquad (A.11)$$

Thus we can state that

$$var(\Lambda) = E(\Lambda^2) - E^2(\Lambda) = \psi^1(L) \qquad (A.12)$$

B. Averages and Variances of POLSAR Covariance Matrix Determinant and Log-Determinant

In this section, the expected value and variance value of these mixture of random variables are derived

$$\chi_L^d \sim \prod_{i=0}^{d-1}\chi(2L - 2i) \qquad (A.13)$$

$$\Lambda_L^d \sim \sum_{i=0}^{d-1}\Lambda(2L - 2i) \qquad (A.14)$$

given the averages and variances of individual components.

$$avg\left[\chi(2L)\right] = 2L \qquad (A.15)$$
$$var\left[\chi(2L)\right] = 4L \qquad (A.16)$$
$$avg\left[\Lambda(2L)\right] = \psi^0(L) + \ln 2 \qquad (A.17)$$
$$var\left[\Lambda(2L)\right] = \psi^1(L) \qquad (A.18)$$

Making use of the mutual independence property of each component X_i, the variance and expectation of the summation and product of random variables can be written as:

$$avg\left(\sum_{i=1}^n X_i\right) = \sum_{i=1}^n avg(X_i),$$
$$var\left(\sum_{i=1}^n X_i\right) = \sum_{i=1}^n var(X_i),$$
$$avg\left(\prod_{i=1}^n X_i\right) = \prod_{i=1}^n avg(X_i),$$
$$var\left(\prod_{i=1}^n X_i\right) = \prod_{i=1}^n\left[avg^2(X_i) + var(X_i)\right] - \prod_{i=1}^n avg^2(X_i).$$

Thus they can be rewritten more usefully as:

$$avg\left[\chi_L^d\right] = 2^d \cdot \prod_{i=0}^{d-1}(L - i),$$
$$var\left[\chi_L^d\right] = \prod_{i=0}^{d-1}4(L-i)(L-i+1) - \prod_{i=0}^{d-1}4(L-i)^2,$$
$$avg\left[\Lambda_L^d\right] = d \cdot \ln 2 + \sum_{i=0}^{d-1}\psi^0(L-i),$$
$$var\left[\Lambda_L^d\right] = \sum_{i=0}^{d-1}\psi^1(L-i)$$

APPENDIX B
DERIVING THE CHARACTERISTIC FUNCTIONS FOR THE CONSISTENT MEASURES OF DISTANCE

Given that the characteristic function (CF) of the elementary log-chi square distributions can be written as

$$CF_{\Lambda(2L)}(t) = 2^{it}\Gamma(L+it)/\Gamma(L)$$

then the CF for the following random variables, which are combinations of the above elementary random variables, can be derived

$$\Lambda_L^d \sim \sum_{i=0}^{d-1}\Lambda(2L-2i)$$

$$\mathbb{L} \sim \Lambda_L^d - d\cdot\ln(2L)$$

$$\mathbb{D} \sim \mathbb{L} - d\cdot\ln L + \sum_{i=0}^{d-1}\psi^0(L-i)$$

$$\mathbb{C} \sim \sum_{i=0}^{d-1}[\Lambda(2L-2i)-\Lambda(2L-2i)]$$

Since we can state that

$$CF_{\sum X_i}(t) = \prod CF_{X_i}(t)$$
$$CF_{x+k}(t) = e^{itk}CF_x(t)$$

then we have:

$$CF_{\Lambda_L^d}(t) = \frac{2^{idt}}{\Gamma(L)^d}\prod_{j=0}^{d-1}\Gamma(L-j+it) \qquad (B.19)$$

$$CF_{\mathbb{L}} = \frac{1}{L^{idt}\Gamma(L)^d}\prod_{j=0}^{d-1}\Gamma(L-j+it) \qquad (B.20)$$

$$CF_{\mathbb{D}} = \frac{1}{\Gamma(L)^d}\prod_{j=0}^{d-1}e^{idt\psi^0(L-j)}\Gamma(L-j+it) \qquad (B.21)$$

Also due to

$$CF_{-\Lambda(2L)}(t) = 2^{-it}\frac{\Gamma(L-it)}{\Gamma(L)}$$
$$\Delta(2L) \sim \Lambda(2L)-\Lambda(2L)$$
$$\Gamma(L-it)\Gamma(L+it) = \Gamma(2L)B(L-it,L+it)$$
$$CF_{\Delta(2L)}(t) = \frac{\Gamma(2L)B(L-it,L+it)}{\Gamma^2(L)}$$

then we arrive at:

$$CF_{\mathbb{C}} = \prod_{j=0}^{d-1}\frac{\Gamma(2L-2j)B(L-j-it,L-j+it)}{\Gamma^2(L-j)} \qquad (B.22)$$

with $\Gamma()$ and $B()$ denoting Gamma and Beta functions respectively.

APPENDIX C
SAR INTENSITY AS A SPECIAL CASE OF POLSAR COVARIANCE MATRIX DETERMINANT

In this appendix, the following results for SAR intensity I are shown to be special cases of the results given in this paper for the determinant of the POLSAR covariance matrix $det|C_v|$.

Specifically, the following results extend from the authors previous work on single-look SAR [15], i.e. $d = L = 1$, which is considerd a special case. We can state the following:

$$I \sim \bar{I}\cdot pdf\left[e^{-R}\right] \qquad (C.23)$$

$$\log_2 I \sim \log_2\bar{I} + pdf\left[2^{D-2^D}\right] \qquad (C.24)$$

$$\frac{I}{\bar{I}} = \mathbb{R} \sim pdf\left[e^{-R}\right] \qquad (C.25)$$

$$\log_2 I - \log_2\bar{I} = \mathbb{D} \sim pdf\left[2^D e^{-2^D}\ln 2\right] \qquad (C.26)$$

$$\log_2 I_1 - \log_2 I_2 = \mathbb{C} \sim pdf\left[\frac{2^c}{(1+2^c)^2}\ln 2\right] \qquad (C.27)$$

$$avg(\mathbb{D}) = -\gamma/\ln 2 \qquad (C.28)$$

$$var(\mathbb{D}) = \frac{\pi^2}{6}\frac{1}{\ln^2 2} \qquad (C.29)$$

$$mse(\mathbb{D}) = \frac{1}{\ln^2 2}(\gamma^2+\pi^2/6) = 4.16 \qquad (C.30)$$

but also the following well-known results are considered for multi-look SAR, i.e. $d=1, L>1$:

$$I \sim pdf\left[\frac{L^L I^{L-1}e^{-LI/\bar{I}}}{\Gamma(L)\bar{I}^L}\right] \qquad (C.31)$$

$$N = \ln I \sim pdf\left[\frac{L^L}{\Gamma(L)}e^{L(N-\bar{N})-Le^{N-\bar{N}}}\right] \qquad (C.32)$$

It will be shown that all of these results are special cases of the result derived previously and rewritten below:

$$|C_v| \sim \frac{|\Sigma_v|}{(2L)^d}\prod_{i=0}^{d-1}\chi^2(2L-2i) \qquad (C.33)$$

$$\ln|C_v| \sim \ln|\Sigma_v| + \sum_{i=0}^{d-1}\Lambda(2L-2i)-d\cdot\ln 2L \qquad (C.34)$$

$$\frac{|C_v|}{|\Sigma_v|} = \mathbb{R} \sim \frac{1}{(2L)^d}\prod_{i=0}^{d-1}\chi^2(2L-2i) \qquad (C.35)$$

$$\ln|C_v| - \ln|\Sigma_v| = \mathbb{D} \sim \sum_{i=0}^{d-1}\Lambda(2L-2i)-d\cdot\ln 2L \qquad (C.36)$$

$$\ln|C_{1v}| - \ln|C_{2v}| = \mathbb{C} \sim \sum_{i=0}^{d-1}\Delta(2L-2i) \qquad (C.37)$$

$$avg(\mathbb{D}) = \sum_{i=0}^{d-1}\psi^0(L-i)-d\cdot\ln L \qquad (C.38)$$

$$var(\mathbb{D}) = \sum_{i=0}^{d-1}\psi^1(L-i) \qquad (C.39)$$

$$mse(\mathbb{D}) = \left[\sum_{i=0}^{d-1}\psi^0(L-i)-d\cdot\ln L\right]^2 + \sum_{i=0}^{d-1}\psi^1(L-i) \qquad (C.40)$$

This appendix also derives new results for multi-look SAR data, which can be thought of either as extensions of the corresponding single-look SAR results or as simple cases of

the POLSAR results presented above. They are:

$$\frac{I}{\bar{I}} = \mathbb{R} \quad \sim \quad \frac{1}{2L}\chi^2(2L) \tag{C.41}$$

$$\ln I - \ln \bar{I} = \mathbb{D} \quad \sim \quad \Lambda(2L) - \ln 2L \tag{C.42}$$

$$\ln I_1 - \ln I_2 = \mathbb{C} \quad \sim \quad \Delta(2L) \tag{C.43}$$

$$avg(\mathbb{D}) \quad = \quad \psi^0(L) - \ln L \tag{C.44}$$

$$var(\mathbb{D}) \quad = \quad \psi^1(L) \tag{C.45}$$

$$mse(\mathbb{D}) \quad = \quad \left[\psi^0(L) - \ln L\right]^2 + \psi^1(L) \tag{C.46}$$

The derivation process detailed below consists of two-phases. The first phase collapses the generic multi-dimensional POLSAR results into the classical one-dimensional SAR domain. Mathematically this means setting the dimensional number in POLSAR to $d = 1$ and collapsing the POLSAR covariance matrix into the variance measure in SAR, which also equals the SAR intensity i.e. $|C_v| = I, |\Sigma_v| = \bar{I}$.

The output of the first phase, in the general case, is applicable to multi-look SAR data, where $d = 1$ but $L > 1$. The second phase simplifies the multi-look results into single-look results, which will match those presented in our previous work [15]. Mathematically, it means setting $L = 1$ in the multi-look result and converting from the natural logarithmic domain used in this paper to the base-2 logarithm used in [15] (base-2 was chosen in the previous paper to simplify the computation).

A. Original Domain: SAR Intensity and its ratio

Setting $d = 1$, $|C_v| = I$ and $|\Sigma_v| = \bar{I}$ into Eqns. C.33 and C.35 we find that:

$$I \quad \sim \quad \frac{\bar{I}}{2L}\chi^2(2L)$$

$$\frac{I}{\bar{I}} = \mathbb{R} \quad \sim \quad \frac{1}{2L}\chi^2(2L)$$

Or in PDF forms, and applying the variable change theorem,:

$$\frac{2LI}{\bar{I}} \quad \sim \quad pdf\left[\frac{x^{L-1}e^{-x/2}}{2^L\Gamma(L)}\right]$$

$$\frac{I}{\bar{I}} \quad \sim \quad pdf\left[\frac{x^{L-1}e^{-x/2}}{2^L\Gamma(L)} \cdot dx/dt\right]_{x=2L\cdot t}$$

$$\sim \quad pdf\left[\frac{L^L t^{L-1}e^{-Lt}}{\Gamma(L)}\right]$$

$$I \quad \sim \quad pdf\left[\frac{L^L t^{L-1}e^{-Lt}}{\Gamma(L)} \cdot dt/dx\right]_{t=x/\bar{I}}$$

$$\sim \quad pdf\left[\frac{L^L x^{L-1}e^{-Lx/\bar{I}}}{\bar{I}^L\Gamma(L)}\right]$$

Thus we have the following results for multi-look SAR:

$$I \quad \sim \quad pdf\left[\frac{L^L x^{L-1}e^{-Lx/\bar{x}}}{\bar{I}^L\Gamma(L)}\right] \tag{C.47}$$

$$\frac{I}{\bar{I}} = \mathbb{R} \quad \sim \quad pdf\left[\frac{L^L x^{L-1}e^{-Lx}}{\Gamma(L)}\right] \tag{C.48}$$

Now setting $L = 1$, these results become:

$$I \quad \sim \quad pdf\left[\frac{e^{x/\bar{I}}}{\bar{I}}\right] \tag{C.49}$$

$$\frac{I}{\bar{I}} = \mathbb{R} \quad \sim \quad pdf\left[e^{-x}\right] \tag{C.50}$$

which is the same as stated in [15], demonstrating that the previous work is a special case of the more generic POLSAR forms.

B. Log-transformed domain: SAR log-intensity and the log-distance

The result for multi-look SAR data written in the log-transformed domain can be derived from two different approaches. The first is to follow a simplification method, where the results for log-transformed POLSAR data are simplified into log-transformed multi-look SAR results.

The second approach is to apply log-transformation to the results derived in the previous section. In this section, it is shown that both approaches would result in identical results.

Setting $d = 1$, $|C_v| = I$ and $|\Sigma_v| = \bar{I}$ into Eqns. C.34 and C.36 we have

$$\ln I \quad \sim \quad \ln \bar{I} + \Lambda(2L) - \ln 2L$$

$$\ln I - \ln \bar{I} = \mathbb{L} \quad \sim \quad \Lambda(2L) - \ln 2L$$

Or in PDF form, and applying the variable change theorem we have:

$$\ln I - \ln \bar{I} + \ln 2L \quad \sim \quad pdf\left[\frac{e^{Lx-e^x/2}}{2^L\Gamma(L)}\right]$$

$$\ln I - \ln \bar{I} \quad \sim \quad pdf\left[\frac{e^{Lx-e^x/2}}{2^L\Gamma(L)} \cdot dx/dt\right]_{x=t+\ln 2L}$$

$$\sim \quad pdf\left[\frac{L^L e^{Lt-Le^t}}{\Gamma(L)}\right]$$

$$\ln I \quad \sim \quad pdf\left[\frac{L^L e^{Lt-Le^t}}{\Gamma(L)} \cdot dt/dx\right]_{t=x-\ln \bar{I}}$$

$$\sim \quad pdf\left[\frac{L^L e^{L(x-\bar{N})-Le^{x-\bar{N}}}}{\Gamma(L)}\right]$$

with $\bar{N} = \ln \bar{I}$. Thus the first approach arrives at

$$\ln I = \mathbb{N} \quad \sim \quad pdf\left[\frac{L^L e^{L(x-\bar{N})-Le^{x-\bar{N}}}}{\Gamma(L)}\right] \tag{C.51}$$

$$\ln I - \ln \bar{I} = \mathbb{L} \quad \sim \quad pdf\left[\frac{L^L e^{Lt-Le^t}}{\Gamma(L)}\right] \tag{C.52}$$

In the second approach, log-transformation is applied on previous results for multi-look SAR intensity and its ratio in the original domain (Eqns. C.48 and C.47). This also arrives at the same results shown above, however the detailed working is omitted for brevity.

To compute summary statistics for the multi-look SAR dispersion, set $d = 1$ into Eqns. C.40, C.38 and C.39 we

have:

$$
\begin{aligned}
avg(\mathbb{L}) &= \psi^0(L) - \ln L \\
var(\mathbb{L}) &= \psi^1(L) \\
mse(\mathbb{L}) &= \left[\psi^0(L) - \ln L\right]^2 + \psi^1(L)
\end{aligned}
$$

This completes the first phase of the derivation process. The second phase of simplification involves setting $L = 1$ into the above results for multi-look SAR data, and converting natural logarithm into base-2 logarithm. First, setting $L = 1$ makes the above results become:

$$
\begin{aligned}
\ln I = \mathbb{N} &\sim pdf\left[e^{(x-\bar{N})-e^{x-\bar{N}}}\right] \\
\ln I - \ln \bar{I} = \mathbb{L} &\sim pdf\left[e^{x-e^x}\right] \\
avg(\mathbb{L}) &= \psi^0(1) = -\gamma \\
var(\mathbb{L}) &= \psi^1(1) = \pi^2/6 \\
mse(\mathbb{L}) &= \left[\psi^0(1)\right]^2 + \psi^1(1) = \gamma^2 + \pi^2/6
\end{aligned}
$$

with γ denoting the Euler-Mascharoni constant. Then to convert to base-2 logarithm from natural logarithmic transformation, we again use the variable change theorem. That is:

$$
\begin{aligned}
\log_2 I = \mathbb{N}_2 &\sim pdf\left[e^{(x-\bar{N})-e^{x-\bar{N}}} \cdot dx/dt\right]_{x=t\cdot\ln 2} \\
\mathbb{N}/\ln 2 = \mathbb{N}_2 &\sim pdf\left[e^{(t\cdot\ln 2-\bar{N})-e^{t\cdot\ln 2-\bar{N}}}\ln 2\right]_{\bar{N}_2=\bar{N}\cdot\ln 2} \\
&\sim pdf\left[2^{t-\bar{N}_2}e^{2^{t-\bar{N}_2}}\ln 2\right]
\end{aligned}
$$

$$
\begin{aligned}
\log_2 I - \log_2 \bar{I} = \mathbb{L}/\ln 2 = \mathbb{L}_2 &\sim pdf\left[e^{x-e^x}\right]_{x=t\cdot\ln 2} \\
&\sim pdf\left[2^t e^{2^t}\ln 2\right]
\end{aligned}
$$

$$
\begin{aligned}
avg(\mathbb{L}_2) &= avg(\mathbb{L})/\ln 2 = -\gamma/\ln 2 \\
var(\mathbb{L}_2) &= var(\mathbb{L})/\ln^2 2 = \frac{\pi^2}{6}\frac{1}{\ln^2 2} \\
mse(\mathbb{L}_2) &= mse(\mathbb{L})/\ln^2 2 = \frac{1}{\ln^2 2}(\gamma^2 + \pi^2/6) = 4.1161
\end{aligned}
$$

C. Deriving the PDF for SAR dispersion and contrast

The PDF for SAR dispersion can be easily derived from the PDF for the log-distance given above as:

$$
\ln I - avg(\ln I) = \mathbb{D} \sim pdf\left[\frac{e^{L[x+\psi^0(L)]-Le^{x+\psi^0(L)-\ln L}}}{\Gamma(L)}\right] \tag{C.53}
$$

due to $d = 1$ and

$$
\begin{aligned}
\mathbb{D} &\sim \mathbb{L} - avg(\mathbb{L}) \\
avg(\mathbb{L}) &= \psi^0(L) - \ln L \\
\mathbb{L} &\sim pdf\left[\frac{L^L e^{Lt-Le^t}}{\Gamma(L)}\right]
\end{aligned}
$$

Setting $L = 1$ for Single-Look SAR we have

$$
\mathbb{D} \sim pdf\left[e^{x-\gamma-e^{x-\gamma}}\right] \tag{C.54}
$$

due to: $\psi^0(1) = -\gamma$ and $\Gamma(1) = 1$ with γ being the Euler Mascheroni constant (which equals 0.5772). In base-2 logarithm domain, invoking the variable change theorem:

$$
\begin{aligned}
\mathbb{D}_2 &= \log_2 I - avg(\log_2 I) = \mathbb{D}/\ln 2 \\
\mathbb{D}_2 &\sim pdf\left[e^{x-\gamma-e^{x-\gamma}} \cdot \frac{dx}{dt}\right]_{x=t\cdot\ln 2}
\end{aligned}
$$

Thus we have

$$
\mathbb{D}_2 \sim pdf\left[e^{-(2^x e^{-\gamma})}(2^x e^{-\gamma})\ln 2\right] \tag{C.55}
$$

which is consistent with the results found in our previous work [15].

Setting $d = 1$ into Eqn. for contrast results in

$$
\ln I_1 - \ln I_2 = \mathbb{C} \sim \Delta(2L) \tag{C.56}
$$

The characteristic function would then be

$$
CF_{\mathbb{C}} = \frac{\Gamma(2L)B(L-it, L+it)}{\Gamma(L)^2} \tag{C.57}
$$

Thus the PDF can be written as

$$
\mathbb{C} \sim pdf\left[\frac{\Gamma(2L)}{\Gamma(L)^2}\frac{e^{Lx}}{(1+e^x)^{2L}}\right] \tag{C.58}
$$

due to

$$
\begin{aligned}
CF_{\mathbb{C}}(x) &= \frac{\Gamma(2L)}{\Gamma(L)^2}B(1/(1+e^x), L-it, L+it) \\
&= \frac{\Gamma(2L)}{\Gamma(L)^2}\int_0^{1/(1+e^x)} z^{L-it-1}(1-z)^{L+it-1}dz \\
\frac{\partial}{\partial x}CF_{\mathbb{C}}(x) &= \frac{\partial CF_{\mathbb{C}}(x)}{\partial 1/(1+e^x)} \cdot \frac{\partial 1/(1+e^x)}{\partial x} \\
&= e^{itx}\frac{\Gamma(2L)}{\Gamma(L)^2}\frac{e^{Lx}}{(1+e^x)^{2L}}
\end{aligned}
$$

Setting $L = 1$ into Eqn. C.58 we have the PDF for contrast of single-look SAR data:

$$
\mathbb{C} \sim pdf\left[\frac{e^x}{(1+e^x)^2}\right] \tag{C.59}
$$

Converting to base-2 logarithm gives the following:

$$
\begin{aligned}
\mathbb{C}/\ln 2 = \mathbb{C}_2 &\sim pdf\left[\frac{e^x}{(1+e^x)^2} \cdot dx/dt\right]_{x=t\cdot\ln 2} \\
&\sim pdf\left[\ln 2\frac{2^t}{(1+2^t)^2}\right]
\end{aligned}
$$

which is also consistent to the results shown in our previous work [15].

REFERENCES

[1] K. Conradsen, A. Nielsen, J. Schou, and H. Skriver, "A test statistic in the complex Wishart distribution and its application to change detection in polarimetric SAR data," *IEEE Transactions on Geoscience and Remote Sensing*, vol. 41, no. 1, pp. 4 – 19, Jan 2003.

[2] V. Alberga, G. Satalino, and D. K. Staykova, "Comparison of polarimetric SAR observables in terms of classification performance," *International Journal of Remote Sensing*, vol. 29, no. 14, pp. 4129–4150, 2008. [Online]. Available: http://www.tandfonline.com/doi/abs/10.1080/01431160701840182

[3] I. Joughin, D. Winebrenner, and D. Percival, "Probability density functions for multilook polarimetric signatures," *Geoscience and Remote Sensing, IEEE Transactions on*, vol. 32, no. 3, pp. 562 –574, may 1994.

[4] J.-S. Lee, K. Hoppel, S. Mango, and A. Miller, "Intensity and phase statistics of multilook polarimetric and interferometric SAR imagery," *IEEE Transactions on Geoscience and Remote Sensing*, vol. 32, no. 5, pp. 1017 –1028, Sep 1994.

[5] R. Touzi and A. Lopes, "Statistics of the stokes parameters and of the complex coherence parameters in one-look and multilook speckle fields," *Geoscience and Remote Sensing, IEEE Transactions on*, vol. 34, no. 2, pp. 519 –531, mar 1996.

[6] C. Lopez-Martinez and X. Fabregas, "Polarimetric SAR speckle noise model," *Geoscience and Remote Sensing, IEEE Transactions on*, vol. 41, no. 10, pp. 2232–2242, 2003.

[7] E. Erten, "The performance analysis based on SAR sample covariance matrix," *Sensors (Basel)*, vol. 12, no. 3, pp. 2766–2786, 2012.

[8] J.-S. Lee, M. Grunes, and G. de Grandi, "Polarimetric SAR speckle filtering and its implication for classification," *IEEE Transactions on Geoscience and Remote Sensing*, vol. 37, no. 5, pp. 2363 –2373, Sep 1999.

[9] J. S. Lee, M. R. Grunes, and R. Kwok, "Classification of multi-look polarimetric SAR imagery based on complex Wishart distribution," *International Journal of Remote Sensing*, vol. 15, no. 11, pp. 2299–2311, 1994.

[10] S. N. Anfinsen, R. Jenssen, and T. Eltoft, "Spectral clustering of polarimetric SAR data with Wishart-derived distance measures," in *3rd International Workshop on Science and Applications of SAR Polarimetry and Polarimetric Interferometry*, vol. 3, Jan 2007.

[11] P. Kersten, J. S. Lee, and T. Ainsworth, "Unsupervised classification of polarimetric synthetic aperture radar images using fuzzy clustering and EM clustering," *IEEE Transactions on Geoscience and Remote Sensing*, vol. 43, no. 3, pp. 519 – 527, Mar 2005.

[12] K. Y. Lee and T. Bretschneider, "Derivation of separability measures based on central complex Gaussian and Wishart distributions," in *IEEE Internationaal Geoscience and Remote Sensing Symposium (IGARSS), 2011*, Jul 2011, pp. 3740 –3743.

[13] F. Cao, W. Hong, Y. Wu, and E. Pottier, "An unsupervised segmentation with an adaptive number of clusters using the SPAN/H/α/A space and the complex Wishart clustering for fully polarimetric SAR data analysis," *IEEE Transactions on Geoscience and Remote Sensing*, vol. 45, no. 11, pp. 3454 –3467, Nov 2007.

[14] N. R. Goodman, "The distribution of the determinant of a complex Wishart distributed matrix," *Annals of Mathematical Statistics*, vol. 34, no. 1, pp. 178–180, 1963.

[15] T. H. Le, I. V. McLoughlin, K. Y. Lee, and T. Brestchneider, "SLC SAR speckle filtering using homoskedastic features of logarithmic transformation," in *Proceedings of the 31st Asian Conference on Remote Sensing (ACRS)*, Hanoi, Vietnam, Nov 2010.

[16] R. Raney and G. Wessels, "Spatial considerations in SAR speckle consideration," *IEEE Transactions on Geoscience and Remote Sensing*, vol. 26, no. 5, pp. 666 –672, Sep 1988.

[17] S. Anfinsen, A. Doulgeris, and T. Eltoft, "Estimation of the equivalent number of looks in polarimetric synthetic aperture radar imagery," *IEEE Transactions on Geoscience and Remote Sensing*, vol. 47, no. 11, pp. 3795 –3809, Nov 2009.

[18] "AIRSAR implementation," [Accessed Feb 2013]. [Online]. Available: http://airsar.jpl.nasa.gov/documents/genairsar/chapter3.pdf

[19] "RadarSat-2 product description," [Accessed Feb 2013]. [Online]. Available: http://gs.mdacorporation.com/products/sensor/radarsat2/RS2_Product_Description.pdf

[20] A. Freeman and S. Durden, "A three-component scattering model for polarimetric SAR data," *IEEE Transactions on Geoscience and Remote Sensing*, vol. 36, no. 3, pp. 963 –973, May 1998.

[21] S. Cloude and E. Pottier, "An entropy based classification scheme for land applications of polarimetric SAR," *IEEE Transactions on Geoscience and Remote Sensing*, vol. 35, no. 1, pp. 68 –78, Jan 1997.

[22] J. Schou, H. Skriver, A. Nielsen, and K. Conradsen, "CFAR edge detector for polarimetric SAR images," *IEEE Transactions on Geoscience and Remote Sensing*, vol. 41, no. 1, pp. 20 – 32, Jan 2003.

[23] T. H. Le and I. V. McLoughlin, "SAR Fuzzy-MLE speckle filter using the distance consistency property in homoskedastic log-transformed domain," in *Proceedings of the 32nd Asian Conference on Remote Sensing (ACRS)*, Taipei, Taiwan, Nov 2011.

[24] F. Medeiros, N. Mascarenhas, and L. Costa, "Evaluation of speckle noise MAP filtering algorithms applied to SAR images," *International Journal of Remote Sensing*, vol. 24, no. 24, pp. 5197–5218, Dec 2003.